

Impact of changing location and power of a PV system in electrical distribution networks, integrating MATLAB and OpenDSS

Javier Andrés Ruíz-Garzón, Daniel José González-Tristancho & Francys Catalina Espinosa-González

Programa de Ingeniería Eléctrica, Escuela Colombiana de Ingeniería Julio Garavito, Colombia. javier.ruiz@escuelaing.edu.co, daniel.gonzalez@escuelaing.edu.co, francy.espinosa@mail.escuelaing.edu.co

Received: November 15th, 2017. Received in revised form: March 16th, 2018. Accepted: April 3rd, 2018.

Abstract

This paper presents the electrical impact of connecting a photovoltaic (PV) system without storage to the electric distribution network 13-bus IEEE test case, integrating MATLAB and OpenDSS using a fluctuated vector of irradiance as an input for the PV system. The capacity of the primary source is reduced to a value where the system requires to add PV modules to provide a reliable source of power. PV modules are placed in both source bus and buses affected by voltage drops. Then, PV source is progressively increased to evaluate the voltage variations when combining PV and conventional sources. The results showed how a reduction in the generation affects the voltage levels of the system and how the inclusion of PV modules located in specific nodes tend to recover the system.

Keywords: solar power generation; power system simulation; OpenDSS; photovoltaic modules; IEEE test cases; irradiance.

Impacto del cambio de la ubicación y la potencia de un sistema FV en redes de distribución eléctrica, integrando MATLAB y OpenDSS

Resumen

Este artículo presenta el impacto eléctrico de conectar un sistema fotovoltaico (FV) sin almacenamiento a la red de distribución IEEE de 13 nodos, mediante la integración de MATLAB y OpenDSS utilizando un vector de irradiancia fluctuante como entrada para el sistema fotovoltaico. La capacidad de la fuente primaria se reduce a un valor en el que el sistema requiere agregar módulos fotovoltaicos para proporcionar una fuente confiable de electricidad. Los módulos fotovoltaicos se colocan tanto en el nodo fuente como en los nodos afectados por caídas de tensión. Luego, la fuente fotovoltaica se incrementa progresivamente para evaluar las variaciones de tensión al combinar fuentes fotovoltaicas y convencionales. Los resultados mostraron cómo una reducción en la generación afecta los niveles de tensión del sistema y cómo la inclusión de módulos fotovoltaicos ubicados en nodos específicos tiende a recuperar el sistema.

Palabras clave: generación de energía solar; simulación de sistemas de potencia; OpenDSS; módulos fotovoltaicos; caso de prueba IEEE; irradiancia.

1. Introduction

Solar radiation is defined as the energy coming from the sun as electromagnetic waves; incident solar power over a surface is known as solar irradiance, measured in $[W/m^2]$ and the solar energy corresponds to incident solar power over a surface on a period of time in $[Wh/m^2]$ [1].

The generation of electricity from solar radiation, namely photovoltaics, is directly proportional to the incident radiation on the photovoltaic panels and depends on the

geographical area where they are located, the season of the year, cloudiness, among other climatic and environmental factors, in addition to the technical and constructive characteristics of the panels [2].

Solar irradiance fluctuates throughout the day and its impact on the distribution grid is an important issue regarding the effect of variable irradiance on large-scale application of photovoltaic systems [3]. The growth of the energy demand leads to the use of photovoltaic (PV) modules as an alternative to conventional sources. The use of this non-

conventional type of renewable energy must fulfill the requirements established by the Colombian Mining and Energy Planning Unit (UPME for its acronym in Spanish) in law 1715 of 2014 [4], regarding the rational use of energy and renewable resources.

Under Resolution 121 of 2017 from the Energy and Gas Regulatory Commission (CREG for its acronym in Spanish) [5], the activities concerned to small scale self-generation (up to 1 MW) and large-scale distributed generation (up to 5 MW) are regulated. It was established that the installed power capacity must be equal or below 5 % of the distribution circuit nominal capacity. With CREG's Resolution 030 of 2018 [6], the capacity of the distributed generators was increased up to 15%, promoting the use of renewable energies.

However, the use of photovoltaic systems to supply the growing demand may create some electrical issues because it is a DC source; it is converted to an AC signal; it needs to be synchronized to the grid; and, even most importantly, it does not provide a steady energy source. Therefore, the technical issues of replacing generators in the IEEE 13 node test system with a photovoltaic system are analyzed, working with a variable irradiance provided by the Institute of Hydrology, Meteorology, and Environmental Studies of Colombia (IDEAM for its acronym in Spanish) [7]. The power from both sources, renewable and conventional energy, are gradually changed to supply the system loads, in accordance to the power quality requirements regarding voltage sags and swells for PV systems included in standards IEEE STD 1547-1,2003 [8], ANSI C84.1-2006 [9], and CREG 024-2005 [10], for voltage variations allowed in Colombia. This study has been done using the EPRI open source software OpenDSS through a MATLAB interface that allows working with time-variable irradiance which is processed by OpenDSS to provide the required outputs.

This paper is organized as follows: the second section presents the integration of MATLAB and OpenDSS tools for modeling of distribution networks with PV systems. The third section shows the results of simulating an IEEE 13-bus test case system, including a PV generation embedded in the OpenDSS model. In the fourth section, obtained results and their analyses are presented. Finally, the conclusions are shown.

2. Modelling PV systems under variable irradiance

Earlier studies [11,12] have shown the influence of variable irradiance and temperature on the Maximum Power Point Tracking (MPPT) on PV systems, leading to a change, usually a decrease of the energy output, which impacts the operation of the entire grid.

2.1. Modelling PV systems

A PV array consists of PV cells connected in either series or parallel and its mathematical model can be expressed as follows [13,14]:

$$P_{cc,inv} = P_{cc,fov}(1 - L_{cab}) \quad (1)$$

$$P_{cc,fov} = P_o R_{to,var} [1 - g(T_c - 25)] \frac{E}{1000} \quad (2)$$

$$T_c = T_{amb} + (TONC - 20) \frac{E}{800} \quad (3)$$

Where $P_{cc,fov}$ is the DC power output from the PV panels; L_{cab} is the power losses at the DC wiring between the PV panels and the inverter input (including fuse losses, switches, wirings, antiparallel diodes if any, etc.); E is the solar irradiance; g is the temperature coefficient of power in $1/^\circ\text{C}$; T_c is the temperature of solar cells; T_{amb} is the room temperature in the shade; $TONC$ is the nominal operating temperature of the module, P_o is the nominal power of the generator; and $R_{to,var}$ is the performance which includes the percentages of losses due to the photovoltaic modules operating at normal condition.

PV modules can be mathematically modeled as follows [13]:

$$I_o = n_p I_{ph} - n_p I_{rs} \left(\exp \left(k_o \frac{V}{n_s} \right) \right) \quad (4)$$

Where, I_o is the PV array output current; V is the PV output voltage; I_{ph} is the cell photocurrent, proportional to solar irradiation; I_{rs} is the cell reverse saturation current that depends on the temperature; k_o is related to Boltzmann constant; n_p is the numbers of parallel strings in the PV array and n_s is the numbers of series strings in the PV array.

Using Equations (1) - (4), the output power versus output voltage curve can be obtained (Fig. 1) [11].

2.2. PV Systems under Variable Irradiance

Previous works, based on the fluctuation of irradiance and temperature, have shown that such variability modifies the maximum power point (MPP) making the flux of energy unstable [15].

Solar irradiance depends on several meteorological parameters such as air temperature (T), relative humidity (RH), wind speed (Ws), wind direction (Wd), cloudiness (Cl), sunshine duration (S), clearness index (Kt), pressure (P), etc., and geographical coordinates such as latitude and longitude. Another study [16] illustrates that irradiance can be predicted; but its results comes from measured data in a specific weather station located at El Dorado International Airport in Bogotá, Colombia [7].

One of the main issues of PV systems without stable irradiance is the reliability of the data, considering that this kind of analysis requires a minimum amount of data for a 24-hour period as previous work shows [15].

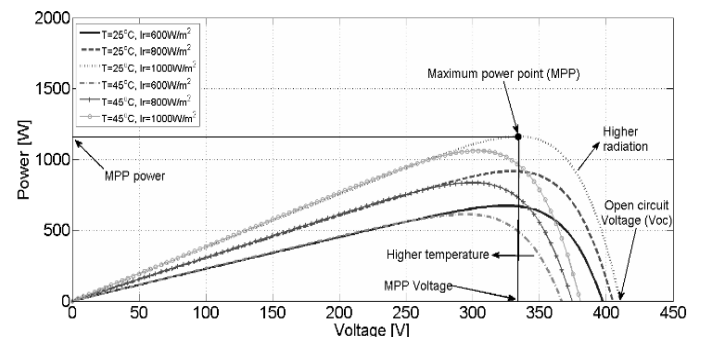


Figure 1. Power vs voltage curve of a photovoltaic system
Source: Adapted from [11].

The exponential growth of renewable resources has created the requirement of more accurate PV system models. There are several studies proposing and validating MPPT techniques such as *perturb and observe*, *incremental conductance*, *current sweep*, and *constant voltage* [11]. Since this paper does not focus on the MPPT, MPP placement is not considered, even though irradiance will be a variable.

According to standards IEEE STD 1547-2003 [8] and ANSI C84.1-2006 [9], which establish parameters for distribution systems working under a 60Hz frequency, this study considered the fact that irradiance and temperature lead to changes in voltage levels. Such changes are within the acceptable voltage variations found in the abovementioned standards.

2.3. Modelling variable irradiance using OpenDSS

OpenDSS can simulate power systems with the key advantage of modeling different types of variable conditions such as irradiance and loads. The frequency of the input data determines the time range of the simulation; for instance, if the input data is acquired every half an hour, the results shall be displayed as a function of this interval. Considering the active power, either supplied or absorbed by a specific bus bar, the results will be shown using the same rate of the input data. It is important to mention that all the data could be acquired from physical metering devices such as a pyrometer for irradiance. These data are normally obtained and displayed as a vector, which contains the required information that allows the software to run the simulations. To guarantee power flow convergence, there must be consistency among the quantity of data used and vector size.

OpenDSS models variable irradiance by working with vectors that can be introduced directly as a variable (vector type) or called from an Excel file, saved as a comma-separated values (CSV) file.

Once the requirements for vectors are fulfilled, the vector is called to OpenDSS using a simple line code which has five parts: the irradiance vector with any desirable name (*MyIrrad* for example); the number of points used and the time frame between each point specified; the command to call the vector with the actual name found in the CSV; and finally, the *useActual* command which represents the data entered as a per unit value.

To run the simulation, the user must ensure that all CVS files used and the OpenDSS script are in the same folder with the data vector either introduced as a line vector code or written as numbers separated by a single space.

3. Modelling distribution networks in OpenDSS

In this study, the 13-bus IEEE test case included in OpenDSS is used, the code was developed by students from Tennessee Technological University [17].

The general single-line diagram is shown in Fig. 2, and it is given by the IEEE-PES, divided in voltages nodes [18] to represent the general system. Initially, bus 632 is connected to a voltage regulator and from this to the source or node 650 which OpenDSS adopts it as a slack node.

According to the official test case from IEEE [19], a validation was required to ensure that power flow results in terms of voltage and currents evaluated in the nodes of the

system were accurate. This revision led to a correction on the library code in element 603 which represents a line that connects nodes 632-645 and 645-646, as shown below.

Figs. 3 to 5 show that such correction has a relevant effect in the line impedances. Fig. 3 indicates the initial code for line 603 and Fig. 4 shows the information given by IEEE regarding the same power line. Comparing those two figures, a typographical error is observed due to the first and last value from both resistance and reactance are shifted. The correction is shown in Fig. 5.

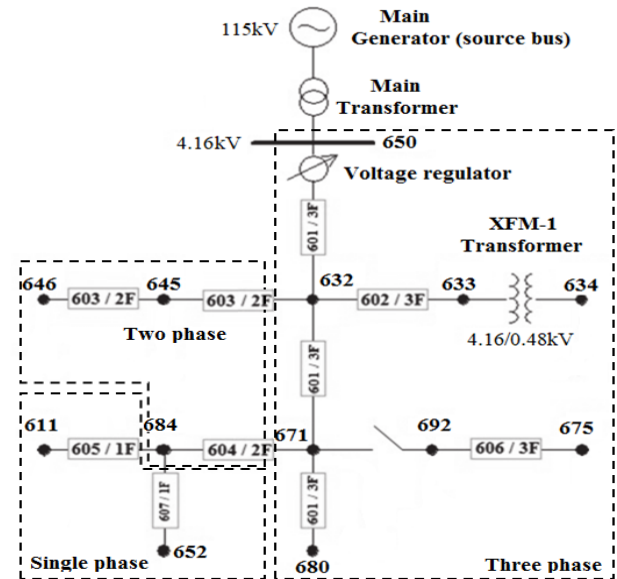


Figure 2. Modified IEEE 13 Node test feeder
Source: Adapted from [19]

```
New linecode.mtx603 nphases=2
~ rmatrix = (1.3238 | 0.2066 1.3294 )
~ xmatrix = (1.3569 | 0.4591 1.3471 )
~ units=mi
```

Figure 3. Original code line at the Tennessee Tech students' script
Source: [17]

Configuration 603:					
Z (R +jX) in ohms per mile					
0.0000	0.0000	0.0000	0.0000	0.0000	0.0000
			1.3294	1.3471	0.2066 0.4591
					1.3238 1.3569

Figure 4. Impedance matrix configuration for line 603 given by IEEE
Source: The authors

```
New linecode.mtx603 nphases=2
~ rmatrix = (1.3294 | 0.2066 1.3238)
~ xmatrix = (1.3471 | 0.4591 1.3569)
~ units=mi
```

Figure 5. Corrected line code used for the original script
Source: The authors

4. Integration of MATLAB and OpenDSS for the modelling

4.1. Linking together MATLAB and OpenDSS

To improve the results' user-friendliness obtained by OpenDSS, it is possible to establish a link between OpenDSS and MATLAB following the flowchart shown in Fig. 6. It is important to clarify that all power flows are carried out by OpenDSS calling Excel files. These files contain the environmental resources such as irradiance or temperature while MATLAB displays the results and gives the users the opportunity to modify those parameters in real time.

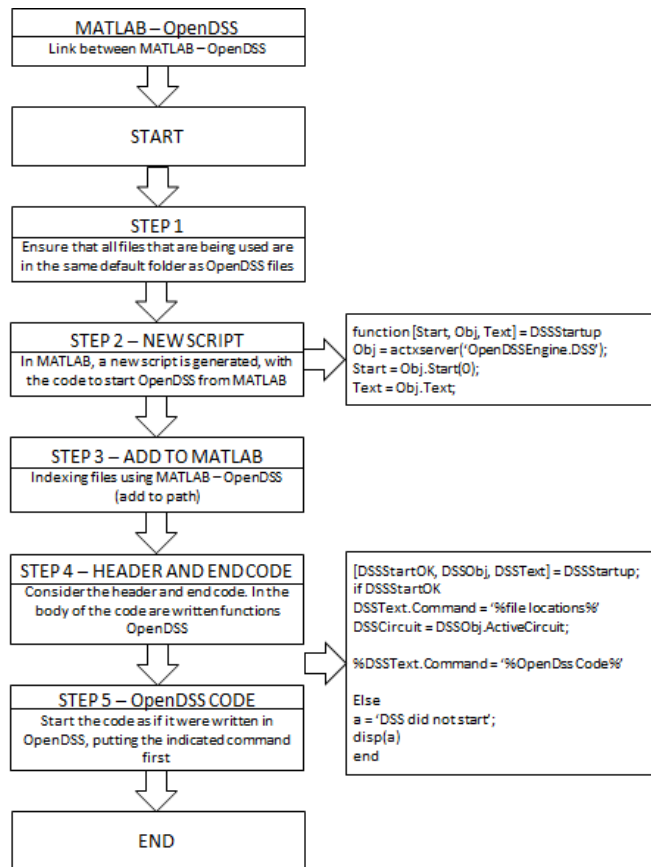


Figure 6. Flowchart to connect OpenDSS with MATLAB
Source: The authors

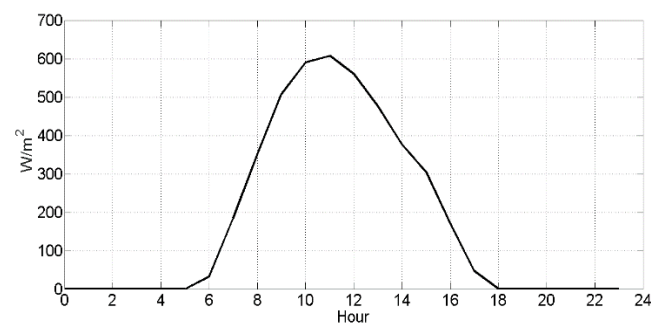


Figure 7. Irradiance using MATLAB and OpenDSS
Source: The authors

Table 1.
Utilization voltage limits according to ANSI C84.1-1 of 2006

Utilization voltage limits		
	Optimal voltage range	Acceptable voltage range
Minimum	90%	86.7%
Maximum	105%	105.8%

Source: [9]

Following the previous flowchart, OpenDSS can be linked using any C-based programming language software such as Python or LabVIEW.

4.2. Evaluating OpenDSS results using MATLAB

According to the data provided by IDEAM [7], an Excel file was called to OpenDSS as explained in section *Modelling variable irradiance using OpenDSS*. The raw data were used as input for the model and the information is presented in this study as a daily irradiance curve generated by MATLAB, as shown in Fig. 7.

There are other advantages for using a connection between OpenDSS and MATLAB, mainly the visualization of results, since MATLAB allows to display the charts with a range variety of options.

5. Case study

The study is divided into four stages. In the first one, the total power from the source bus is gradually decreased to assess the effect of voltage drops in different buses according to the power flow. A reduction of 16.68% in the total power system led to voltage levels in several nodes to drop below the acceptable voltage range (0.867 pu, according to Table 1).

In the second stage, a PV array is added in the source bus to compensate the changes in the system using 680 kVA. Then, in the third stage of the study, the response of the system adding a greater PV capacity of 1360 kVA in the source bus is analyzed. A fourth stage of the study is considered shifting the location from source bus to a distant node of the network to assess the effect in voltage levels.

Since a PV system is added, the information used must be real and accurate; therefore, a KC85TS High Efficiency Multicrystal Photovoltaic Module has been selected [20] and the array has been calculated using Eqs. (1) - (4) to fit the needs of the different stages of the study. Considering that the irradiance of January 2014 is the highest and most unwavering registered in [7], it is used as an input to evaluate the behavior of the system.

All stages for this study are done with a variable measured irradiance, therefore the variation in voltage levels of the system is affected.

Originally, the critical buses were found while decreasing the power generated by the main source; the IEEE 13 node test feeder is connected to the grid, which virtually acts as an "infinite source". This source needs to be changed to a regular generator or a synchronous machine to be able to control its power capacity. To make this happen, both generator and grid must be modeled under the same conditions. Same initial results are guaranteed.

With the synchronous machine installed in the model a power flow was conducted and a selection of the altered

Table 2.
Service voltage limits according to ANSI C84.1-1 of 2006

Service voltage limits		
	Optimal voltage range	Acceptable voltage range
Minimum	97.5%	95%
Maximum	105%	105.8%

Source: [9]

Table 3.
Bus voltages for 16.68% of total power reduction

Bus/Node	Phase	VLN [kV]	Angle [degrees]	VLN [pu]	Base [kV]
675	1	2.0216	15	0.8417	4.16
	2	2.3144	-101.1	0.96361	4.16
	3	1.9761	136.5	0.82278	4.16
611	3	1.9711	136.2	0.82068	4.16
684	1	2.0319	15.2	0.84602	4.16
	3	1.9756	136.4	0.82254	4.16

Source: The authors

buses is made based on those that were below 90% of its nominal value or over 110% as CREG 024-2005 [10] establishes, and those that go under the values allowed by ANSI C84.1-2006 for service and utilization voltage levels, as shown in Table 1 and Table 2 [9].

6. Results and analysis

An analysis of the power flows considering the stages of the study were carried out for the different scenarios previously described. Results of the power flows lead to determine that the most critical outputs were obtained in the nodes 611 (single-phase), 684 (two-phase) and 675 (three-phase). The evaluation of the impact of installing PV arrays on certain buses shows that the voltage in the system is compensated.

Table 3 shows the results of voltage level in the most critical nodes with a reduction of 16.68% in the total power system. Voltage drops below 86.7% in the buses are highlighted following the criteria allowed by ANSI C84.1-2006 [9].

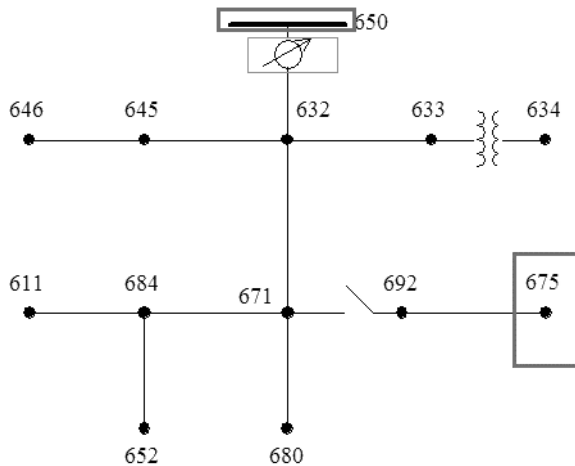


Figure 8. Modified IEEE 13 Node test feeder
Source: The authors

Table 4.
Bus voltages with a PV array of 680 kVA in the source bus

Bus/Node	Phase	VLN [kV]	Angle [degrees]	VLN [pu]	Base [kV]
675	1	2.0831	14.1	0.86731	4.16
	2	2.407	-101.6	1.0022	4.16
	3	2.0326	135.8	0.84629	4.16
611	3	2.0274	135.5	0.84411	4.16
684	1	2.0939	14.3	0.87183	4.16
	3	2.032	135.7	0.84602	4.16

Source: The authors

Table 5.
Bus voltages with a PV array of 1360 kVA in the source bus

Bus/Node	Phase	VLN [kV]	Angle [degrees]	VLN [pu]	Base [kV]
675	1	2.0831	14.1	0.86731	4.16
	2	2.407	-101.6	1.0022	4.16
	3	2.0326	135.8	0.84629	4.16
611	3	2.0274	135.5	0.84411	4.16
684	1	2.0939	14.3	0.87183	4.16
	3	2.032	135.7	0.84602	4.16

Source: The authors

In the first case, when the total power of the system is reduced, all nodes have voltage drops below 86.7%. The most critical case between three-phase nodes is at bus 675 as showed in Fig. 8, in which the third phase drops to 0.82278 pu, as seen in Table 3, despite the largest drop in the voltage occurring in the single-phase bus 611 with a value of 0.82068 pu.

Table 4 presents the results when a PV array is added in the source bus trying to compensate the changes in the system using 680 kVA. Under these conditions, the inclusion of the PV array in the source bus shows an increase in the voltage levels of the system, however these levels are still below the allowed limits.

A greater PV array capacity of 1360 kVA installed in the source bus led to results showed in Table 5, which shows how the system recovers acceptable voltage levels by duplicating the PV array capacity installed in the source bus.

During the last stage of the analysis, the PV array of 1360kVA is shifted from source bus to a distant three-phase node of the network (675). Results are showed in Table 6.

Finally, a greater impact is observed when a power PV capacity of 1360 kVA is installed in the most critical three-phase node. The difference between installing this PV capacity in the 675 node, rather than the source bus, represents an increase from 0.8728 pu to 0.9021 pu for the voltage in the third phase.

Table 6.
Bus voltages with a PV array of 1360 kVA in bus 675

Bus	Phase	VLN [kV]	Angle [degrees]	VLN [pu]	Base [kV]
675	1	2.213	19.7	0.92138	4.16
	2	2.516	-95.4	1.0476	4.16
	3	2.1667	141.8	0.90213	4.16
611	3	2.1499	141.3	0.89515	4.16
684	1	2.2119	19.8	0.92094	4.16
	3	2.1549	141.5	0.8972	4.16

Source: The authors

It is important to highlight that in the second, third and fourth stages of the study the behavior analyzed in the 611, 684 and 675 nodes can be seen in the rest of the nodes.

As expected, installing more PV capacity in the most critical node can generate a positive impact, trying to recover the system as shown in Table 6.

The previous results open the possibility of performing other simulations in different tools for load flows, to carry out verifications of the veracity of the simulations of distribution networks with PV systems in OpenDSS and MATLAB.

7. Conclusions

The electrical impact of connecting a photovoltaic (PV) system without storage to an existing electric distribution network has been described. Modeling power systems in OpenDSS allows to modify the capacity of generation in parallel with PV penetration considering variable inputs in a time basis interval transforming the standard distribution network into a distributed generation network.

As expected, the synchronous machine installed in the system affected the voltage levels in the nodes when the power capacity is reduced. Overexciting occurs when the power in the generator decreases, because of a higher load requisition, leading to a voltage decrease in the nodes, which can be compensated installing PV arrays as seen in Tables 4, 5 and 6.

Prior to the installation of PV arrays, it is important to determine the nodes of the system where a larger impact in the voltage level is evidenced. As shown in Table 6, installing PV arrays in the critical node allows to mitigate the voltage drops increasing from 0.8228 pu to 0.9021 pu for the voltage in the third phase of node 675.

Historic data regarding irradiance or variable loads can be used as vector inputs without any hardware in the loop configuration to run time-varying conditions in power systems. The integration of OpenDSS and MATLAB allows not only to visualize results but also to modify and iterate them under new conditions in the system.

References

- [1] National Renewable Energy Laboratory [NREL]. Concentrating solar power- best practices handbook for the collection and use of solar resource data, 2010, [Online] Available at: <https://www.nrel.gov/docs/fy10osti/47465.pdf>
- [2] Boyle, G., Renewable energy power for a sustainable future. Third edition. Amersham, UK: Oxford University Press, 2012.
- [3] Woyte, A., Van Thong, V., Belmans, R. and Nijs, J., Voltage fluctuations on distribution level introduced by photovoltaic systems, IEEE Transactions on Energy Conversion, 21 (1), pp. 202-209, 2006, DOI: 10.1109/TEC.2005.845454
- [4] Unidad de Planificación Minero Energética [UPME]. Ley 1715 DE 2014, "Por medio del cual se regula la integración de las energías renovables no convencionales al sistema energético nacional", 2014, [Online]. Available at: http://www.upme.gov.co/Normatividad/Nacional/2014/LEY_1715_2014.pdf
- [5] Comisión de Regulación de Energía y Gas [CREG]. Resolución 121 de 2017 por la cual se ordena hacer público el proyecto de resolución "Por la cual se regulan las actividades de autogeneración a pequeña escala y de generación distribuida en el sistema interconectado nacional", 2017 [Online]. Available at: <http://apolo.creg.gov.co/Publicac.nsf/1c09d18d2d5ffb5b05256eee00709c02/b5341fbcb96db80525819b006d42fa?OpenDocument>
- [6] Comisión de Regulación de Energía y Gas [CREG]. Resolución 030 de 2018 "Por la cual se regulan las actividades de autogeneración a pequeña escala y de generación distribuida en el sistema interconectado nacional", 2018 [Online]. Available at: [http://apolo.creg.gov.co/Publicac.nsf/1c09d18d2d5ffb5b05256eee00709c02/83b41035c2c4474f05258243005a1191/\\$FILE/Creg030-2018.pdf](http://apolo.creg.gov.co/Publicac.nsf/1c09d18d2d5ffb5b05256eee00709c02/83b41035c2c4474f05258243005a1191/$FILE/Creg030-2018.pdf)
- [7] Instituto de Hidrología, Meteorología y Estudios Ambientales de Colombia [IDEAM]. Atlas de radiación solar, ultravioleta y ozono de Colombia, 2016. [Online]. Available at: <http://atlas.ideam.gov.co/visorAtlasRadiacion.html>
- [8] Institute of Electrical and Electronics Engineers [IEEE]. Standard for Interconnecting Distributed Resources with Electric Power Systems. (Std 1547-2003), 2003. [Online]. Available at <http://ieeexplore.ieee.org/document/1225051/>
- [9] American National Standards Institute, Inc. [ANSI]. American national standard for electric power systems and equipment — voltage ratings (60 Hertz). (C84.1-2006), 2006. [Online]. Available at: <https://www.nema.org/Standards/ComplimentaryDocuments/Contents-and-Scope-ANSI-C84-1-2011.pdf>
- [10] Comisión de Regulación de Energía y Gas [CREG]. Resolución 024-2005, "Por la cual se modifican las normas de calidad de la potencia eléctrica aplicables a los servicios de Distribución de Energía Eléctrica", 2005. [Online]. Available at: [http://apolo.creg.gov.co/Publicac.nsf/2b8fb06f012cc9c245256b7b00789b0c/7ef77a545ceb66680525785a007a6b88/\\$FILE/Creg024-2005.pdf](http://apolo.creg.gov.co/Publicac.nsf/2b8fb06f012cc9c245256b7b00789b0c/7ef77a545ceb66680525785a007a6b88/$FILE/Creg024-2005.pdf)
- [11] González, D., Prototipo de energía eléctrica fotovoltaica, para el laboratorio de energía de la Escuela Colombiana de Ingeniería. MSc. thesis, Escuela Colombiana de Ingeniería Julio Garavito, Bogotá, Colombia, 2016.
- [12] Bialasiewicz, J., Renewable energy systems with photovoltaic power generators: operation and modeling. IEEE Transactions on Industrial Electronics, 55, 7, 2752-2758, 2008. DOI: 10.1109/TIE.2008.920583
- [13] Liu, F., Duan, S., Liu, F., Liu, B. and Kang, Y., A variable step size INC MPPT method for PV systems. IEEE Transactions on Industrial Electronics, 55(10074567), pp. 2622-2628, 2008. DOI: 10.1109/TIE.2008.920550
- [14] Instituto para la Diversificación y Ahorro de la Energía [IDAE]. Pliego de condiciones técnicas de instalaciones conectadas a Red, 2011. [Online]. Available at: http://www.idae.es/uploads/documentos/documentos_5654_FV_pliego_condiciones_tecnicas_instalaciones_conectadas_a_red_C20_Julio_2011_3498eaaf.pdf
- [15] Maranda, W. and Piotrowicz, M., Efficiency of maximum power point tracking in photovoltaic system under variable solar irradiance. Bulletin of the Polish Academy of Sciences, Technical Sciences, 62(4), pp. 713-721, 2014. DOI: 10.2478/bpasts-2014-0077
- [16] Mellit, A. and Pavan, A.M., A 24-h forecast of solar irradiance using artificial neural network: Application for performance prediction of a grid-connected PV plant at Trieste, Italy. Solar Energy, 84(5), pp. 807-821, 2010. DOI: 10.1016/j.solener.2010.02.006
- [17] Electric Power Research Institute [EPRI]. Discussion forum for the 13 bus IEEE test case EPRI Distribution System Simulator (OpenDSS) script, 2009. [Online]. Available at: <https://sourceforge.net/p/electricdss/discussion/861977/thread/79ed9387/>
- [18] Nyangoma, J. and Awodele, K., Comparison of different reactive power compensation methods in a power distribution system. Paper presented at the 22nd Southern African Power Universities Engineering Conference, 2014.
- [19] Institute of Electrical and Electronics Engineer [IEEE]. Distribution test feeders, 1992. [Online]. Available at: <http://ewh.ieee.org/soc/pes/dsacom/testfeeders/index.html>
- [20] Kyocera Corporation. KC85TS high efficiency multicrystal photovoltaic module, 2016. [Online]. Available at: <https://www.kyocerasolar.com/dealers/product-center/archives/specsheets/KC85TS.pdf>

J.A. Ruíz-Garzón, received the BSc. Eng in Electrical Engineering in 2012 from the Universidad de la Salle, Bogotá, Colombia, and the MSc degree in

Renewable Energy and Environmental Modelling in 2014 from the University of Dundee, Dundee, Scotland. Currently, he is a full time professor in the Electrical Program at Escuela Colombiana de Ingeniería Julio Garavito, Colombia.
ORCID: 0000-0003-1551-2554

D.J. González-Tristancho, received the BSc. Eng in Electrical Engineering in 2002 and the MSc. degree in Electronic Engineering in 2016, both of them from Escuela Colombiana de Ingeniería Julio Garavito, Bogotá, Colombia. Currently he is a full time professor in the Electrical Program, Escuela Colombiana de Ingeniería Julio Garavito, Colombia.
ORCID: 0000-0003-0905-5019

F.C. Espinosa-González, received the BSc. Eng in Electrical Engineering in 2017 from Escuela Colombiana de Ingeniería Julio Garavito, Colombia.
ORCID: 0000-0001-7823-4788



UNIVERSIDAD NACIONAL DE COLOMBIA

SEDE MEDELLÍN
FACULTAD DE MINAS

Área Curricular de Ingeniería
Eléctrica e Ingeniería de Control

Oferta de Posgrados

Maestría en Ingeniería - Ingeniería Eléctrica

Mayor información:

E-mail: ingelcontro_med@unal.edu.co
Teléfono: (57-4) 425 52 64